Effect of Silicon Nitride (Si3N4) on Mechanical and Dielectric Properties of Fused Silica Ceramic Composites

Pagidi Madhukar (pmadhu88@gmail.com)
National Institute of Technology Andhra Pradesh https://orcid.org/0000-0003-2595-7952
Kishore Kumar Kandi
CVR College Of Engineering - Ibrahimpatan Campus
Gurabvaiah Punugupati
National Institute of Technology Andhra Pradesh
C.S.P. Rao
National Institute of Technology Andhra Pradesh

Research Article

Keywords: Fused Silica, Silicon Nitride, Gelcasting, Flexural strength, Porosity, Dielectric constant, RSM

Posted Date: September 2nd, 2021

DOI: https://doi.org/10.21203/rs.3.rs-845762/v1

Effect of Silicon Nitride (Si_3N_4) on Mechanical and Dielectric Properties of Fused Silica Ceramic Composites

Kishore Kumar Kandi[1]. Gurabvaiah Punugupati[2*]. Pagidi Madhukar[3]. C. S. P. Rao[4].

[1]Department of Mechanical Engineering, CVR College of Engineering, Hyderabad

[2, 3, 4] Department of Mechanical Engineering, National Institute of Technology, Andhra Pradesh

Corresponding Author E-mail: guru.punugupati65@gmail.com **&** pmadhu88@gmail.com

Abstract

Fused silica ceramics composites were widely using for the fabrication of radomes which is the vital component of a missile. The required properties were attained by the addition of small amounts of Silicon Nitride (Si_3N_4) to the fused silica for enhancing flexural strength and without disturbing the dielectric properties. In the present work, porous fused silica ceramic composites were fabricated using gelcasting process, a near net shaping technique. The experiments were conducted using Response Surface Methodology (RSM) central composite with face centered design with six centre points approach. The process parameters of gelcasting process such as solid loading, monomer ratio, monomer content and additive (Si_3N_4) were considered as input parameters and flexural strength, porosity and dielectric constant as response parameters. Single parameter and interaction parameter effect on responses were studied. The effectiveness of derived models was compared with Analysis of Variance (ANOVA) at 95% confidence level. Statistical analysis proven that input parameters have critical effect on responses. The derived RSM mathematical models have a higher R^2 values (Flexural strength 97.62%, Porosity 95.12% and dielectric constant 95.93%) which shows the critical relation between actual and predicted values. The optimal responses obtained were flexural strength 86.173 MPa, porosity 39.767% and dielectric constant 6.949 corresponding parameters process parameters solid loading 47.95%, additive (Si_3N_4) 10.43 wt%, monomer content 15 wt% and monomer ratio 3.

Keywords: Fused Silica, Silicon Nitride, Gelcasting, Flexural strength, Porosity, Dielectric constant, RSM

1. Introduction

Ceramics are highly regarded for their mechanical properties such as strength, durability, and hardness. These are widely used in electronic applications such as semiconductors, conductors, insulators, and magnets due to their electrical and magnetic properties. Advanced ceramics have been progressively used in aerospace, automotive engine, defense, construction, biomedical, nuclear industries, chemical, petrochemical, oil/gas, and industrial wear because of their high strength at elevated temperature, high thermal and chemical stability, low density and high wear resistance. Some applications include space shuttle engine components, tank armor, superconductors and piezoelectric devices [1, 2].

Fused silica is a non-crystalline form of silicon dioxide (quartz, sand) commonly made by fusion of pure silica sand (Wan et al. 2014a) [3]. Nowadays fused silica is one of the essential materials for many engineering and aerospace applications such as radomes, heat shields, antenna window, and crucibles, because of its interesting and prominent properties such as resistant to thermal shock and corrosion, a low thermal expansion coefficient, high softening temperature, a low and stable dielectric constant, and excellent chemical inertness (Haris and Welsh, 1973) [4]. These properties suggest that the SiO_2 ceramics are an ideal candidate material for high-temperature wave-transparent applications and radomes. However, the relatively low mechanical strength of sintered SiO_2 ceramics is inadequate to meet the requirements of advanced re-entry vehicles, especially hypersonic spacecraft. In order to overcome these shortcomings, additives including h-BN, Si_3N_4, fibers, and graphene have been utilized as reinforcements to improve the mechanical strength of ceramics.

Silicon nitride based ceramics are extensively applied in various industrial fields owing to numerous properties, such as high hardness, superior corrosion resistance, excellent mechanical and chemical stability, excellent wear resistance, high decomposition temperature, high strength, and toughness, etc. Si_3N_4 is produced by reacting SiCl with NH_3 (Jong, B.W. et al.,1992) [5]. To attain a high extent of quality, components are spark plasma sintered, hot pressed or reaction sintered as dense parts cannot be produced through direct sintering. At lower temperatures, the bonding of Si_3N_4 particles is attained by addition of sintering aids which normally encourage liquid-phase sintering. Even at elevated temperatures, Si_3N_4 ceramics upholds their strength.

Nowadays, various processing techniques have been developed to prepare both the porous and dense Si_3N_4 ceramics for structural and functional applications (Chen et al., 2010) [6]. These materials can be densified under pressureless sintering conditions by adding a certain amount of sintering aids at high temperatures (1750–2000°C). Si_3N_4 may be well stabilized electrostatically against agglomeration in aqueous slips either at pH of <5 or >9, having either a positive charge or negative charge, respectively (Greil, 1989) [7].

Gelcasting was first developed at Oak Ridge National Laboratory (ORNL) in the 1960s for hard metals and further developed for ceramic materials by combining traditional slip processing with polymer chemistry (Omatete et al., 1991 and Omatete et al., 1997) [8, 9]. The general principle in this process is the ceramic particles suspended are surrounded by a three-dimensional network of the cross-linked polymers. For obtaining maximum solid loading typically a dispersant is used which causes the particles in the ceramic slurry to disperse by means of an electric double layer or steric stabilization. Shrinkage can be minimized during sintering process and dense ceramics can be obtained by high solid loading. The free-radical reaction leads to the formation of micro-gels of monomer and cross-linker inside the suspension, which eventually combine to form a macro-gel network. The gel network formed inside the suspension holds the particles together collectively to mold a dense green body that is demoldable and takes the form of the mold cavity. Molds can be made up of metal or plastic materials that are nonporous (Omatete et al., 1991 and Omatete et al., 1997) [8, 9]. Over the conventional forming methods gelcasting has distinct advantages such as near-net shape fabrication, low contents of organic monomers, high sintered density, and ease of machinability owing to the intensity of homogeneity and high strength (Nojoomi et al., 2014) [10]. Use of non-porous metal or plastic molds that are reusable makes this process economical (Omatete et al., 1991 and Omatete et al., 1997) [8, 9].. Gelcasting has more advantages such as the products produced are consistently defect free, uniformly dense and very strong, and able to form very large parts compared with other forming processes. Gelcasting is attractive for fabricating complex shapes such as radomes, turbine rotors, gears etc.

Wan et. al., (2014) [11] fabricated silica ceramics with high strength, low porosity, low dielectric constant and low dielectric loss by gelcasting using a low-toxicity *N'*,*N*-dimethyl acrylamide (DMAA) gel system. Investigations were done on the properties of green and

sintered ceramics, effect solid loading on the rheology of the slurry. The maximum flexural strength obtained for green bodies and sintered ceramics at a solids loading of 64 vol% and 66 vol% were 15.4 Mpa and 67.4 Mpa. The dielectric constant and low dielectric loss obtained at a solid loading of 64 vol% were 3.27 and 7.82×10^{-4} (at 1 MHz). Wan et. al., (2014a) [3] fabricated fused silica ceramics with excellent properties by gelcasting using *N'*,*N*-dimethylacrylamide, a low toxic gel system. The results were compared with 2-hydroxyethyl methacrylate and toxic acrylamide systems. Investigations were done on the properties such as thermal shock resistance, mechanical and dielectric properties and effects of sintering temperature on the microstructure. The maximum flexural strength was as high as 81.32 Mpa at 1275 °C and after thermal shock at 600°C, the residual flexural strength was reduced. Excellent properties were obtained at 1250°C with the similar flexural strength of 67.43 Mpa and 65.45 Mpa (after thermal shock), the dielectric constant of 3.34, and the low dielectric loss of 1.20×10^{-3} (at 1 MHz). Wan et. al. (2014b) [12] made an attempt using a natural and non-toxic gel, glutinous rice flour as a binder in the gelcasting of fused silica glass. It was found that glutinous rice flour performed exceptionally in the gelcasting process. Fused silica green bodies with 3 wt% glutinous rice flour have a flexural strength of 11.87 Mpa and those sintered at 1275 °C has a flexural strength of 40.02 Mpa with a bulk density of 1.75 g/cm^3. Manivannan et. al. (2013) [13] used colloidal silica as a binder to develop an aqueous gelcasting for fused silica ceramics. It was found that the slurry with a maximum solid loading of 73 vol% with a viscosity of 0.70Pa.s is suitable for gelcasting. The maximum flexural strength of green and sintered samples was found to be 9 Mpa and 65 Mpa with a theoretical density of 88% and 95%. The nano-silica particles of the binder are stuffing the interstitial spots filling the interstitial spots strengthening the mechanical properties in the developed fused silica green body.

Mao et. al. (2006) [14] prepared porous silica ceramics by a starch consolidation casting method. Slurries with various fractions of starch were prepared by ball-milling. The bending strength of the sintered samples varied in the range of 10 Mpa-20 Mpa and the low dielectric constant in the range of 2-2.4 with the porosity of 42%-56%. Lin et. al. (2016) [15] fabricated silicon oxynitride (Si_2N_2O) based wave transparent material with multilayer structures by a two-step sintering route. The effects of atmosphere and temperature on the properties and microstructure of the materials were studied. It was observed that disintegration of Si_2N_2O caused the formation of the multilayer structure. By regulating the disintegration temperature the

thickness of β-Si_3N_4 outer layers and the Si_2N_2O inner layer may perhaps be tailored. The flexural strength of the samples sintered at 1800 °C varied in the range of 210 Mpa-236 Mpa, the dielectric constant < 4.8 and loss tangent < 0.0044. This process allows these ceramic composites to be broadly used as radomes in military applications. Jia et. al. (2003) [16] investigated the mechanical properties of two types of hot-pressed fused silica matrix composites, SiO_2+5 vol.% Si_3N_4 and SiO_2+5 vol.% Si_3N_4+ 10 vol.% C_f. The fracture toughness and ambient strength were significantly improved with the addition of Si_3N_4. The fracture toughness increased sharply from 1.22 to 2.4 Mpa.$m^{1/2}$ by incorporating chopped carbon fibers. The maximum flexural strength of two composites at 1000 °C was found to be 168.9 and 130.6 Mpa which were 77.0 and 77.4% higher than their ambient strength, respectively. Zou et. al. (2012) [17] prepared porous Si_3N_4 ceramics by gelcasting and pressureless sintering and used these as frames for Si_3N_4–SiO_2 composites. By repeating the sol–gel infiltration and sintering process amorphous SiO_2 of different contents were introduced into porous Si_3N_4 frames. Si_3N_4–SiO_2 composites with enhanced thermal shock resistance and mechanical properties were obtained. The flexural strength, fracture toughness, density and dielectric constant of Si_3N_4–SiO_2 composites were increased from 92.6 Mpa, 1.05 Mpam$^{1/2}$, 1.62 g/cm^3 and 2.65 to 148.1 Mpa, 1.70 Mpam$^{1/2}$, 2.18g/cm^3 and 3.61 while the porosity decreased from 49.3% to 22% and the dielectric loss is in the range of $3.23x10^{-3}$ to $3.84x10^{-3}$ with the increase of SiO_2 content from 0 to 25.9 vol%. Li et. al. (2009) [18] developed a novel process to fabricate a porous Si_3N_4–SiO_2 ceramic composite by combining oxidation-bonding with sol–gel infiltration-sintering. The mechanical and dielectric properties of porous Si_3N_4–SiO_2 ceramic composite were enhanced by Sol–gel infiltration and sintering at 1250°C. The flexural strength, porosity, fracture toughness, Vickers hardness, dielectric constant and a dielectric loss were found to be 120 Mpa, 23.9%, 1.4 Mpam$^{1/2}$, 4.1 Gpa, 3.80 and 3.11×10^{-3} (at 14 GHz). Ganesh and Sundararajan (2010) [19] prepared dense β-SiAlON–SiO_2 ceramic composites from β-$Si_4Al_2O_2N_6$ and fused silica varying SiO_2=20, 40, 50, 60, and 80 wt% by sintering at 1500–1750°C for 3–4 h. Thin-wall radomes fabricated by hydrolysis induced aqueous gelcasting (GCHAS) have demonstrated green strengths greater than 20 Mpa. A flexural strength of ~140 Mpa, fracture toughness of 4.2Mpa.$m^{1/2}$, coefficient of thermal expansion of $3.5x10^{-6}$/°C, Young's modulus of 214 Gpa, hardness of 1390 kg/mm^2, dielectric constant of 5.896 and tan δ of 0.002 at 17 GHz was exhibited by silicon oxynitride

formed from a powder mixture of 60 wt% β-$Si_4Al_2O_2N_6$ and 40 wt% SiO_2 sintered at 1750°C for 3 h.

Response surface methodology (RSM) is defined as "a collection of mathematical and statistical techniques useful for the modeling and analysis of problems in which a response (output variable) of interest is influenced by several variables (input variables) and the goal is to optimize the responses that are influenced by the input process parameters" (Montgomery, 2012) [20]. Originally, RSM is developed to model experimental responses and then migrated into the modeling of numerical experiments (Box and Draper, 1987) [21]. They can be applied for modeling and optimization of any engineering problems. Sufficient data is gathered through the experimental design layout and mathematical models for the desired responses as a function of selected variables were developed by applying the multiple regression analysis on the experimental data [22].

2. Materials and Methods

Commercially available SiO_2 (M/s. Ants Ceramics Pvt. Ltd., Thane, India) with an average particle size of 1-5 μm, and Si_3N_4 (M/s. Denka Company Ltd., Japan) with an average particle size of <10 μm are used in this study. Deionized water is used as a solvent. Commercially available dispersants such as Darvan 821A and Darvan C-N (both R.T Vanderbilt, Norwalk, CT), Dolapix A88 and Dolapix CE64 (both Zschimmer & Schwarz, Lahnstein, Germany) are used for dispersing ceramic particles in slurries for obtaining high solid loading and low viscosity. In the process of gelcasting Methacrylamide and *N,N′*- methylenebisacrylamide (both Alfa Aesar) are used as the organic monomer and cross-linker respectively. Ammonium persulfate (APS) and *N,N,N′,N′*-Tetramethylethylenediamine (TEMED) (both Alfa Aesar, United Kingdom) are used as the initiator and catalyst. Surface exfoliation phenomenon green bodies cast in the air was eliminated by adding Polyethylene glycol 400 (Alfa Aesar, United Kingdom). Diluted Nitric acid and Ammonium hydroxide (both S.D. fine chemicals, India) were used for pH adjustment.

3. Slurry preparation

Gelcasting of SiO_2 and Si_3N_4 ceramic composite was carried out at various solid loadings using different monomer content and monomers ratio. A premix solution was prepared by

mixing dispersant (1 wt % of monomer content), surfactant (3 wt % of monomer content), monomers MAM and MBAM (10-15 wt% of solid loading) in distilled water by magnetic stirring. SiO_2 was added to the premix solution and then Si_3N_4 was added in regular intervals for fabrication of SiO_2–Si_3N_4 ceramic composite by gelcasting varied from 5 to 15 wt. % of solid loading and stirred for about 6 hrs and pH of the slurry was adjusted to 11 using diluted Nitric acid and Ammonium Hydroxide.

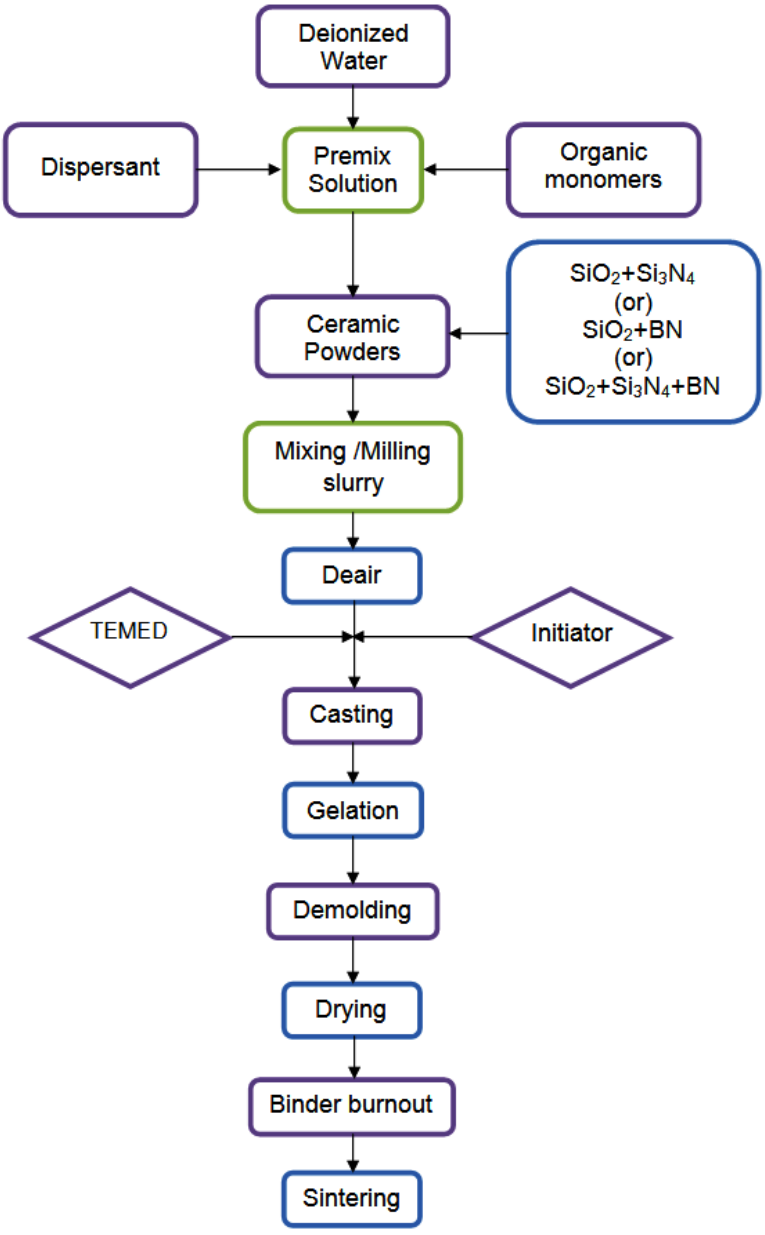

Figure 1. A detailed flowchart of gelcasting process of concern ceramic composite

The slurry was deaired for 15-20 min and then the initiator APS and catalyst TEMED (1 wt % of monomer content) is added for initiation and polymerization. Finally, the slurry was cast into a glass mold and after the monomers had polymerized, the green bodies were demolded. The samples were then dried in a controlled humidity oven for 24 h. Then binder burnout was carried out in a high-temperature furnace at 600 °C for 1 h with a heating rate of 2 °C/min. Then the samples were sintered at 1250 °C with a heating rate of 4 °C/min for 3h in Nitrogen atmosphere. The detailed flowchart of gelcasting process for the preparation of ceramic composite concern i.e. SiO_2–Si_3N_4 shown in Figure 1. Sintered samples of SiO_2–Si_3N_4 ceramic composites were shown in Figure 2.

Figure 2. Sintered samples of SiO_2–Si_3N_4

4. Characterization

4.1. Flexural strength

Flexural strength (Modulus of Rupture) is defined as "the ability of the material to withstand bending forces applied perpendicular to its longitudinal axis". The flexural strength was measured by the three-point flexural method as shown in Figure 3 with a span length of 40 mm and at a crosshead speed of 0.5 mm/min using a universal testing machine as per ASTM-C1161-02C (2006) and is determined as given in Eqn. 1.

$$\sigma_f = \frac{3PL}{2bh^2} \quad (1)$$

where P = fracture load, L = length of support span, b = width of the sample and h = height of the sample.

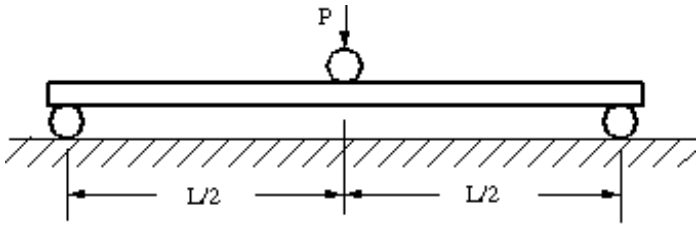

Figure 3. Schematic of three-point bending

4.2 Bulk density and apparent porosity

Bulk density is defined as "the ratio of mass to volume that includes the cavities in a porous material".

$$BD = \frac{DW}{SW_1 - SW_2} X\ \rho \tag{2}$$

Apparent porosity is defined as "the ratio of open pore volume to total volume"

$$AP = \frac{SW_1 - DW}{SW_1 - SW_2} X\ 100 \tag{3}$$

where BD = Bulk Density, AP =Apparent porosity, DW =Dry Weight, SW_1 = Soaked Weight, SW_2 = Suspended weight, ρ = Density of kerosene oil = 0.78 gm/cc

Bulk density and apparent porosity of ceramic bodies were measured by Archimedes principle as per ASTM C373-88(2006) using kerosene as solvent. The specimens were cut into 20 × 20 × 8 mm in size.

Archimedes principle states that "when an object is partially or fully immersed in a fluid it experiences an upward force that is equal to the weight of the fluid displaced by it".

4.3. Dielectric constant and loss tangent

Dielectric constant is defined as "a quantity measuring the ability of a substance to store electrical energy in an electric field".

The dielectric constant can be calculated by Eqn. 4 by measuring the capacitance:

$$K = \epsilon_r' = \frac{cd}{A} = \frac{\varepsilon}{\varepsilon_0} \tag{4}$$

Where K is the dielectric constant; ε_r' is relative permittivity, c is the capacitance; d is the thickness of the specimen; A is the area of the cross-sectional surface; ε is permittivity of the medium; ε_0 is permittivity of free space or vacuum.

5. Results and Discussion

5.1. Zeta potential and pH value

The zeta potential of SiO_2–Si_3N_4 particles in the slurry is studied by varying the dispersant (Darvan 821A) in the range of 0-0.75 wt% as a function of pH value and is depicted in Figure 4.

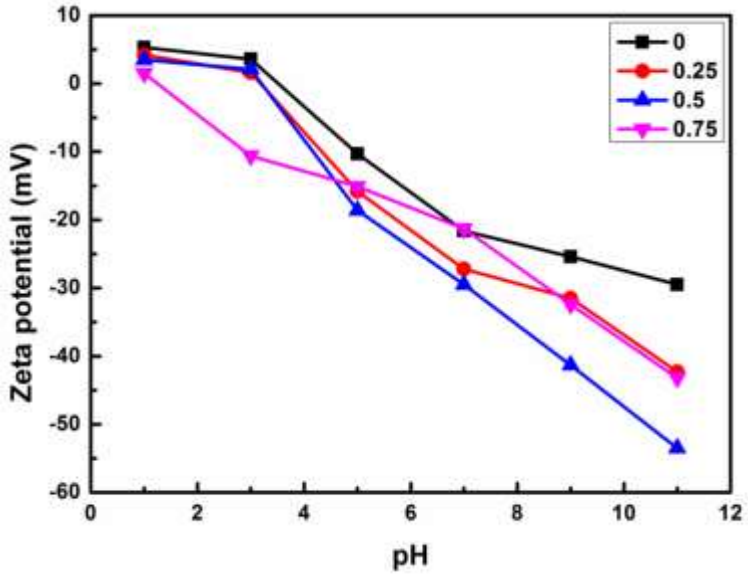

Figure 4. Zeta potential of SiO_2–Si_3N_4 slurries with dispersant Darvan 821A

The zeta potential of SiO_2–Si_3N_4 slurries without dispersant is found to be vary from 5.3 mV at pH 1 to -29.5 mV at pH 11. It can be seen that the isoelectric point (IEP) is at pH 3.8 and the absolute value of zeta potential increases as pH value increases. It is also observed that addition of 0.5 wt% Darvan 821A gives the maximum value of zeta potentials which is about -53.5 mV at pH 11, which is most suitable for obtaining well dispersed SiO_2–Si_3N_4 slurries. The other dispersant levels having good zeta potential other than 0.5 wt% Darvan 821A are 0.75 wt% Darvan 821A and 0.25 wt% Darvan 821A. The corresponding zeta potential values are -43.2 mV and -42.3 mV at pH 11 respectively. The zeta potentials of the remaining slurries are found to be lower and hence not considered.

The pH value of slurry also play an important role on the rheological properties It is observed that high absolute zeta potential value is obtained by increasing the pH value of the slurry which increases the dispersibility of the slurry. The formation of hydroxide layer on the surface of SiO_2 particles is eliminated by the addition of Si_3N_4 particles.

5.2. Solid loading

Higher solid loading of SiO_2–Si_3N_4 slurry is required to improve the mechanical properties of gelcast parts. The solid loading of the slurries are varied from 42 to 50 vol% in which Si_3N_4 content varies from 5 to 15 wt% and remaining is SiO_2. But viscosity increases as the solid loading increases due to agglomeration at higher solid loading which make the slurry difficult to pour into a mold for casting. This is due to flocculation and coagulation caused by the reduction of solvent (water) present in between the ceramic particles. Hence, slurry with 50 vol% solid loading and 15 wt% Si_3N_4 content is suitable for casting into the mold. The variation of viscosity as a function of the shear rate ranging from 0.1–100 s^{-1} for slurries of 50 vol% solids loading and with Si_3N_4 content varying from 5 – 15 wt% is shown in Figure 5.

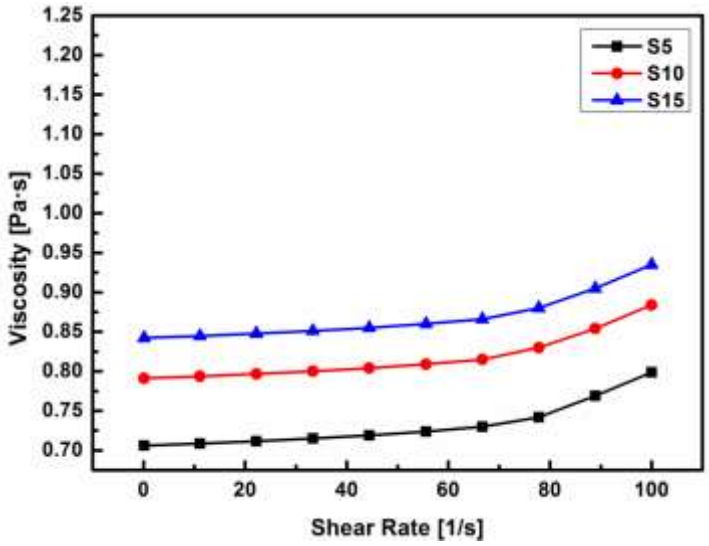

Figure 5. Variation of the viscosity of slurries at various solid loadings

From Figure 5 it can be seen that there is an increase in viscosity from 0.706 to 0.842 Pa.s with an increase in Si_3N_4 content from 5 to 15 wt% and the gel exhibits shear-thickening behavior. The increase in viscosity is due to the agglomeration at high solid loadings.

5.3. X-Ray diffraction analysis and Microstructure

X-ray diffraction patterns of SiO_2–Si_3N_4 ceramic composite sintered at various temperatures are shown in Figure 6. X-ray diffraction analysis is done both on raw ceramics and ceramic composite sintered at 1250 ºC. It can be seen that at 1250 ºC, SiO_2 is transformed into cristobalite phase.

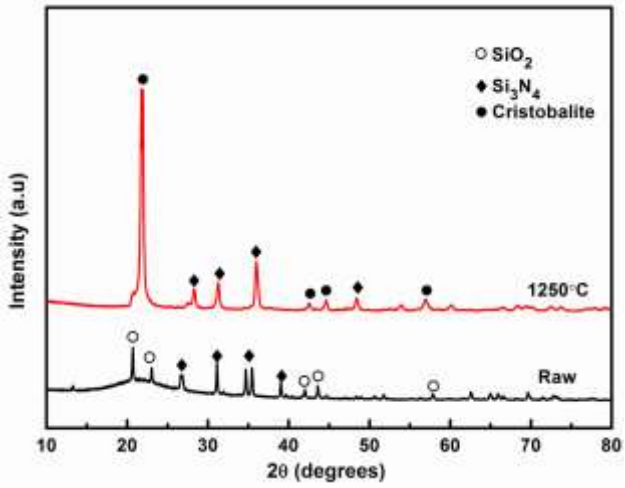

Figure 6. XRD patterns of SiO_2–Si_3N_4 ceramic composite.

The microstructure of sintered SiO_2–Si_3N_4 ceramic composite is shown in Figure 7.

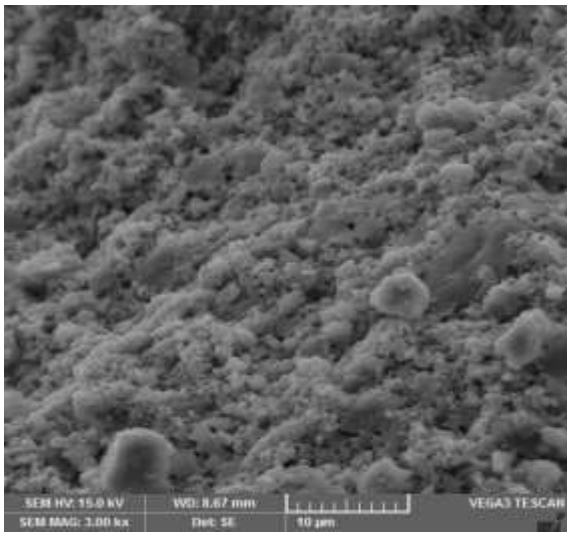

Figure 7. SEM micrograph of sintered SiO_2–Si_3N_4 ceramic composite

5. 4. Results and analysis of SiO_2–Si_3N_4 ceramic composites

5.4.1. Regression model for flexural strength

A regression model for flexural strength of SiO_2–Si_3N_4 ceramic composite is fitted using the experimental results. ANOVA has been applied on the experimental results for flexural strength and the ANOVA results are given in Table 1.

Table 1. ANOVA results for flexural strength.

Source	Sum of Squares	df	Mean Square	F Value	p-value Prob > F	Percentage Contribution
Model	3496.603	8	252.9297	44.09247	< 0.0001	97.598
A-SL	3042.520	1	3042.52	530.3934	< 0.0001	84.924
B-Si_3N_4	311.951	1	311.7505	54.34652	< 0.0001	8.707
C-MC	39.232	1	27.2322	4.747308	0.0457	1.095
D-RM	36.620	1	33.62	5.860874	0.0286	1.022
AB	15.980	1	15.98001	2.785747	0.1158	0.446
BC	8.883	1	8.482656	1.478756	0.2428	0.248
A^2	37.723	1	37.72255	6.576059	0.0216	1.053
C^2	3.696	1	3.695539	0.644232	0.4347	0.103
Residual	86.045	21	5.736346			2.402
Cor Total	3582.649	29				100.00
R-Square: 97.62%		Adjusted R-square: 95.41%		Predicted R-square: 92.39%		

Where A is solid loading (SL), B is Si_3N_4 content, C is monomer content (MC), D is ratio of monomers (RM)

From the above results, it has been observed that SL, Si_3N_4, MC, RM, and SL^2, are significant model terms, and response of each are shown in the Figures 8 (a), (b), (c) and (d) respectively. The regression model generated for flexural strength was given in Eqn. 5 in the coded form.

$$FS = 80.60 + 13A + 4.16B + 1.23C + 1.37D - AB - 0.73BC - 3.82A^2 + 1.19C^2 \qquad (5)$$

From Figure 8 (a) and (b), it is observed that flexural strength increases with solid loading and Si_3N_4 content. Micro-cracks occur in green bodies when the solid loading is low. This may be due to the increase of drying and sintering shrinkages as the space between the particles in the slurry is huge. At low solids loading and Si_3N_4 content the density of the composite decreases during sintering. Therefore, the flexural strength of porous SiO_2–Si_3N_4 sintered ceramic composite is low at lower solids loading and higher the solid loading increases the flexural strength. During sintering, the monomers are burnt out leaving pores. Few pores in the composite will be replaced by the cristobalite which is formed during the sintering. Hence, there is a little significant effect of monomers content and their ratio on the flexural strength of SiO_2–Si_3N_4 ceramic composites as shown in Figure 8 (c) and (d).

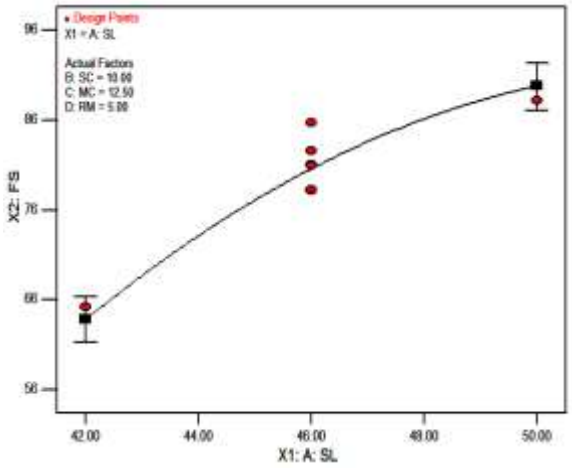

Figure 8 (a). Effect of SL on FS

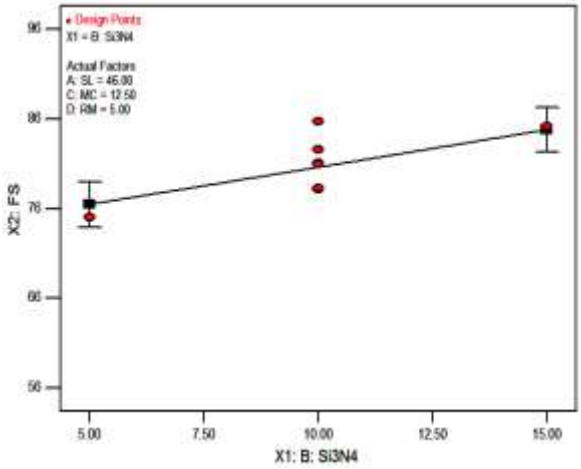

Figure 8 (b). Effect of Si_3N_4 on FS

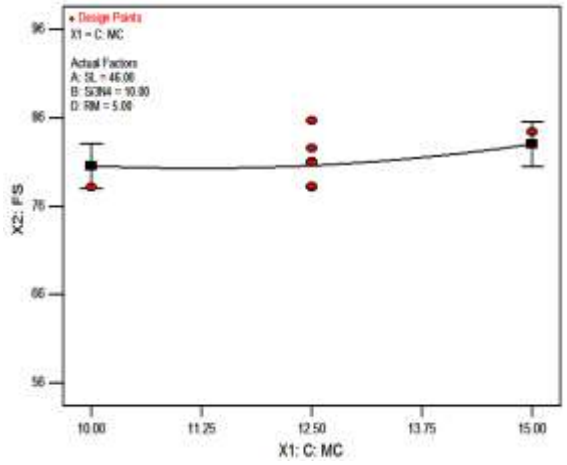

Figure 8 (c). Effect of MC on FS

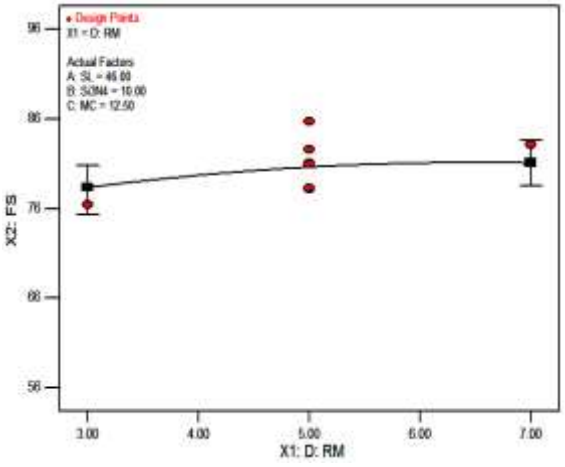

Figure 8 (d). Effect of RM on FS.

Figure 8. Effect of process parameters on flexural strength

5.4.2. Regression model for porosity

A regression model for the porosity of SiO_2–Si_3N_4 ceramic composite is fitted using the experimental results. ANOVA has been applied on the experimental results for porosity and the ANOVA results are given in Table 2.

Table 2. ANOVA results for porosity.

Source	Sum of Squares	df	Mean Square	F Value	p-value Prob > F	Percentage Contribution
Model	158.6867	12	13.22389	27.62487	< 0.0001	95.122
A-SL	105.009	1	105.6089	220.6183	< 0.0001	62.946
B-Si3N4	0.00436	1	0.004356	0.009099	0.9251	0.003
C-MC	17.8802	1	17.8802	37.35197	< 0.0001	10.718
D-RM	8.55601	1	8.556006	17.8736	0.0006	5.129
AB	3.26706	1	3.267056	6.824922	0.0182	1.958
AC	0.79656	1	0.796556	1.664016	0.2143	0.477
AD	0.34516	1	0.345156	0.721036	0.4076	0.207
CD	4.54756	1	4.547556	9.499903	0.0068	2.726
A^2	1.9225	1	1.922496	4.016119	0.0613	1.152
B^2	9.07376	1	9.073755	18.95519	0.0004	5.439
C^2	0.17326	1	0.17326	0.361942	0.5554	0.104
D^2	6.74593	1	6.745934	14.09234	0.0016	4.044
Residual	8.13782	17	0.478695			4.878
Cor Total	166.8245	29				100.00
R-Square: 95.12%		Adjusted R-square: 91.67%		Predicted R-square: 82.75%		

Where A is solid loading (SL), B is Si_3N_4 content, C is monomer content (MC), D is ratio of monomers (RM)

From the above results, it has been observed that SL, MC, RM, interaction of MC and RM, $Si_3N_4^2$, and RM^2 are significant model terms, and response of each is shown in the Figures 9

(a), (b), (c), (d) and (e). The regression model generated for porosity was given in Eqn. 6, in the coded form.

$$Por. = 37.06 - 2.42A - 0.016B - C - 0.69D - 0.45AB + 0.22AC + 0.15AD - 0.53CD - 0.86A^2 - 1.87B^2 + 0.26C^2 + 1.61D^2 \quad (6)$$

In Figure 9 (a), it can be seen that the porosity of sintered body decreases with the increase in solid loading. The ceramic particles are compacted, reducing the pores in the composite with an increase in solid loading. This densifies the ceramic composite. From Figure 9 (b), it is observed that Si_3N_4 content has a significant effect on the porosity. As the Si_3N_4 content increases there is a rise in the porosity and then declines on further addition of Si_3N_4 powder. The rise in the porosity is due to the loose packing of Si_3N_4 particles in SiO_2 ceramics. As the content of Si_3N_4 powder increases the pores in the composite are reduced that increases the density of the composite causing the lower porosity.

The porosity of sintered body increases with monomer content as shown in Figure 9 (c). The pores of sintered body largely initiate from the left over micro-space of the organic polymers in the green body during organic binder burnout. The distribution and intensity of pores depend on the monomer content. Thus more the monomer content more is the porosity in the ceramic body. Figure 9 (d) show the decrease in porosity with the increase of monomers ratio. Higher porosity is obtained on further increase in the monomer ratio. The increase in the ratio of monomers to cross-linker sometimes initiates micro-crack propagation that causes higher porosity. The interaction effects of monomer content and ratio of monomers can be seen in Figure 9 (e).

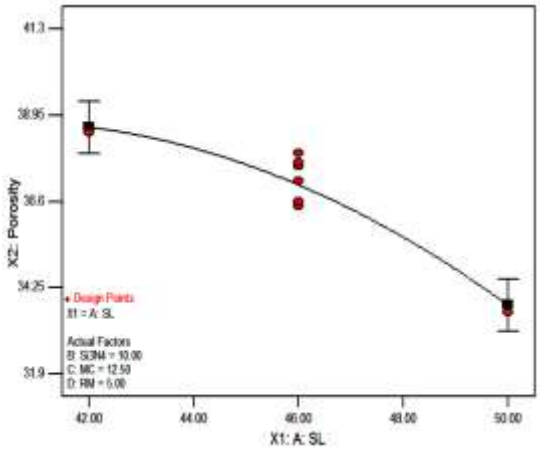

Figure 9. (a). Effect of SL on porosity

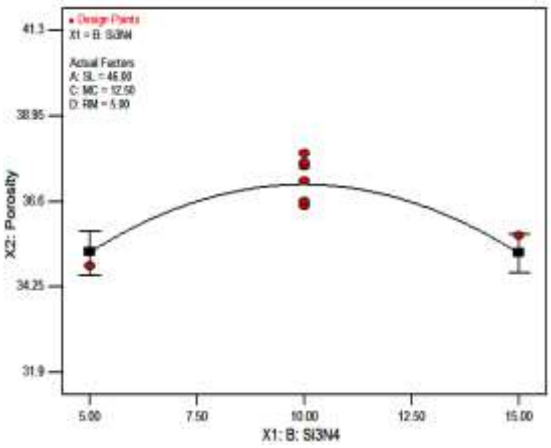

Figure 9. (b). Effect of Si_3N_4 on porosity

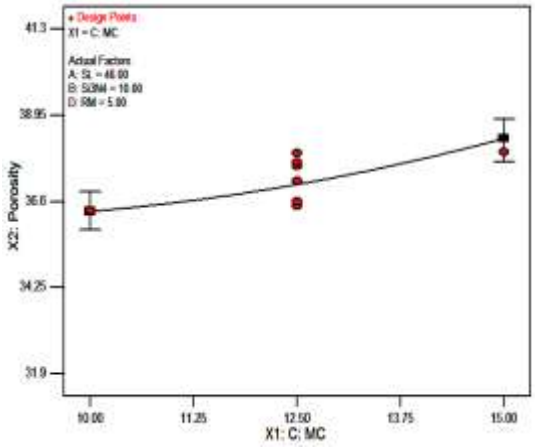

Figure 9 (c). Effect of MC on porosity

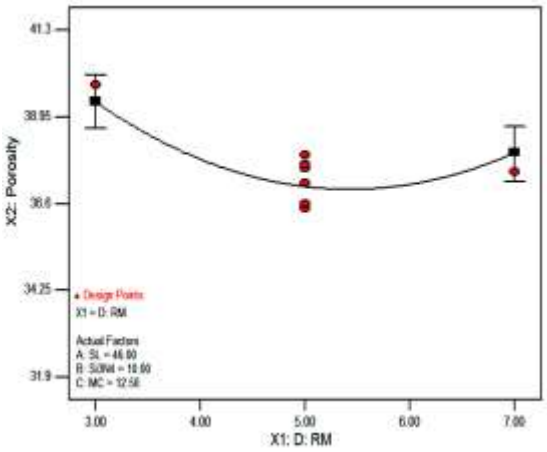

Figure 9 (d). Effect of RM on porosity

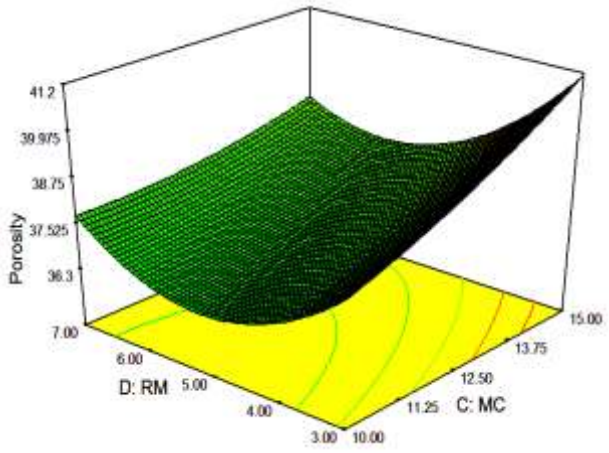

Figure 9 (e). Effect of MC and RM on porosity

Figure 9. Effect of process parameters on porosity

5.4.3. Regression model for dielectric constant

A regression model for dielectric constant of SiO_2–Si_3N_4 ceramic composite is fitted using the experimental results. ANOVA has been applied on the experimental results for dielectric constant and the ANOVA results are given in Table 3.

Table 3. ANOVA results for dielectric constant.

Source	Sum of Squares	df	Mean Square	F Value	p-value Prob > F	Percentage Contribution
Model	4.100	9	0.350244	33.45971	< 0.0001	95.840
A-SL	2.950	1	3.05045	291.4172	< 0.0001	68.969
B-Si3N4	0.001	1	0.000556	0.053074	0.8205	0.013
C-MC	0.339	1	0.338939	32.37969	< 0.0001	7.923
D-RM	0.097	1	0.0968	9.247549	0.0074	2.263
BD	0.074	1	0.074256	7.093888	0.0164	1.736
A^2	0.171	1	0.1708	16.31696	0.0009	3.993
B^2	0.178	1	0.177517	16.95865	0.0007	4.150
C^2	0.039	1	0.039355	3.759641	0.0693	0.920
D^2	0.251	1	0.35134	33.56438	< 0.0001	5.875
Residual	0.178	20	0.010468			4.160
Cor Total	4.278	29				100.00
R-Square: 95.93%		Adjusted R-square: 93.07%		Predicted R-square: 87.36%		

Where A is solid loading (SL), B Si_3N_4 content, C is monomer content (MC), D is ratio of monomers (RM)

From the above results, it has been observed that SL, MC, RM, SL^2, $Si_3N_4^2$, RM^2, interactions of Si_3N_4 and RM, and interactions of Si_3N_4, MC and RM are significant model terms, and are shown in the Figures 10 (a), (b), (c), (d) and (e). The regression model generated for dielectric constant was given in Eqn. 7, in the coded form.

$$DE = 7.40 + 0.04A + 5.556 \times 10^{-3}B - 0.14C + 0.073D + 0.068BD + 0.26A^2 + 0.26B^2 - 0.12C^2 - 0.37D^2 \quad (7)$$

Figure 10 (a) show the increase in density of SiO_2–Si_3N_4 ceramic composite with the increase in solid loading. This will lead to the reduction of pores that causes the increase of dielectric constant. From Figure 10 (b), it can be seen that the dielectric constant initially decreases when Si_3N_4 content is in the range of 5 wt% to 10 wt%. This is due to the increase in the surface area of pores. There is a rise in the dielectric constant on further increasing the Si_3N_4 content from 10 wt% to 15 wt%. This may be due to the increase in the density of the ceramic composite which reduces the transfer of electromagnetic waves through it.

In Figure 10 (c), as the monomer content increases the dielectric constant decreases monotonically. The increase in monomer content decreases the density of sintered ceramic due to the formation of large pores during binder burnout. Thus an increase in the monomer content will lower the density and dielectric properties of ceramics. In Figure 10 (d), it can be observed that the dielectric constant increases as the ratio of monomers increase from 3 to 5. This increase is due to the higher binding effect between the ceramic particles that leads to low pores. Further the dielectric constant decreases as the monomer ratio increases from 5 to 7, due to the excessive binding effect, agglomeration of ceramic particles takes place followed by the formation of micro cracks. The interaction effects of Si_3N_4 content and ratio of monomers on dielectric constant can be seen in Figure 10 (e).

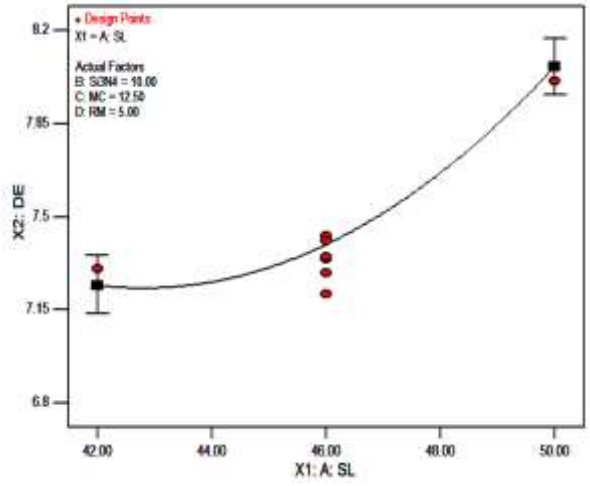

Figure 10 (a). Effect of SL on DE

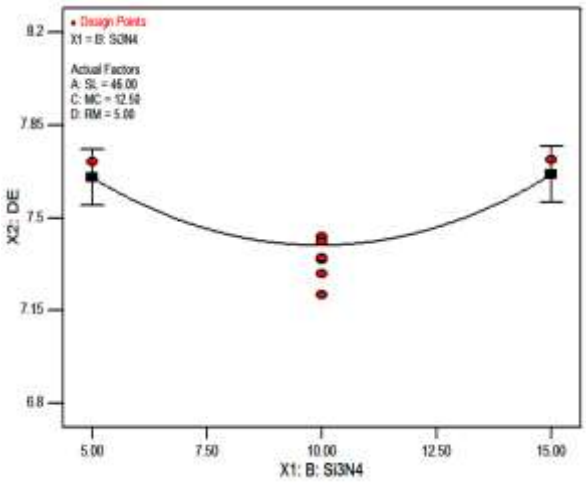

Figure 10 (b). Effects of Si_3N_4 on DE

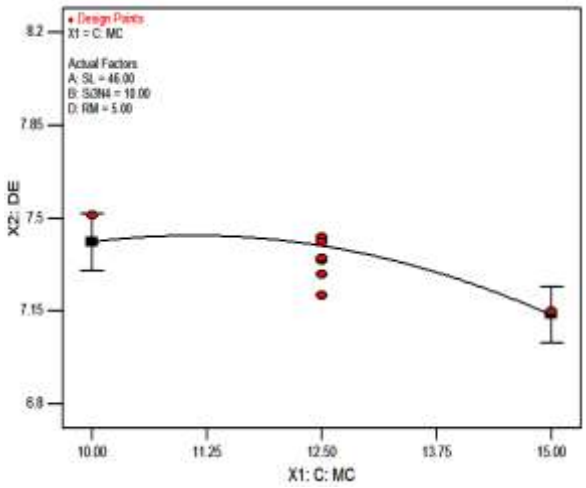

Figure 10 (c). Effect of MC on DE

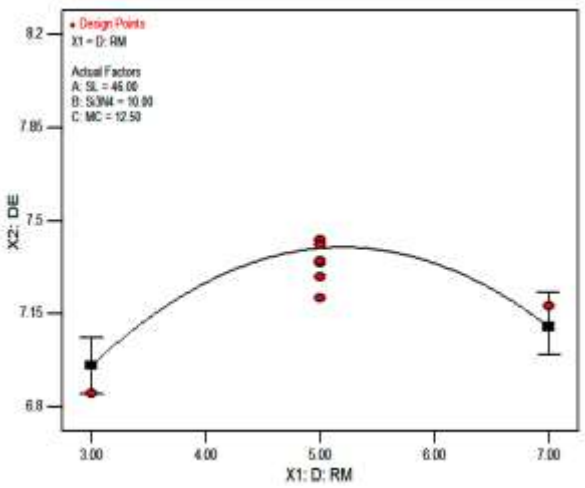

Figure 10 (d). Effect of RM on DE

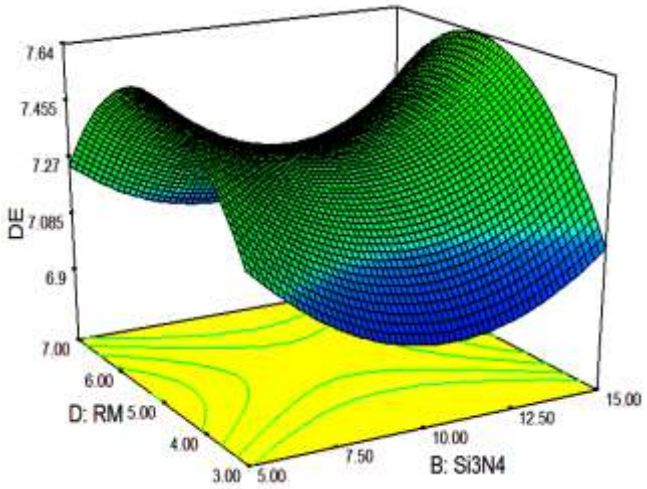

Figure 10 (e). Effect of Si_3N_4 and RM on DE

Figure 10. Effect of process parameters on dielectric constant

5.4.4. Multi-response optimization using desirability function

Multi-response optimization using desirability function was carried out in combination with response surface methodology to surmount the difficulty of inconsistent responses of single response optimization. The range and goals of input parameters i.e. solid loading, monomer content, and ratio of monomers and the responses i.e. flexural strength, porosity and dielectric constant are given in Table 4.

Table 4. Range of input parameters and responses for desirability

Name	Goal	Lower Limit	Upper Limit
A-SL (vol %)	Maximize	42	50
B-Si_3N_4 content (wt %)	in range	5	15
C-MC (wt %)	is in range	10	15
D-RM	is in range	3	7
FS (MPa)	Maximize	56.19	95.12
Por. (%)	Maximize	31.95	41.28
DE	Minimize	6.8	8.14

The aim of optimization is to evaluate the best set of inputs for maximization of flexural strength and porosity, and minimization of dielectric constant. This is indicated by the desirability of RSM analysis. The optimum value of responses is to be chosen for maximum desirability index for various sets of inputs. A set of 10 optimal solutions is derived and tabulated in Table 5 for the particular set of input range (Table 4). The desirability of output responses i.e. flexural strength, porosity and dielectric constant is shown in Figures 11 as ramp graph. The desirability of each parameter and each response and combined parameters are shown in Figures 12 as a bar graph. The overall desirability of the responses is found to be 0.803.

Table 5. Set of optimal solutions for SiO_2–Si_3N_4 ceramic composite.

Number	SL	Si_3N_4	MC	RM	FS	Por.	DE	Desirability
1	47.95	10.43	15	3	86.173	39.767	6.949	0.808
2	47.95	10.33	15	3	86.107	39.777	6.948	0.808
3	47.91	10.34	14.97	3	85.998	39.780	6.947	0.806
4	47.93	11.12	15	3	86.580	39.670	6.957	0.806
5	47.92	11.26	15	3	86.644	39.649	6.958	0.806
6	47.82	11.37	15	3	86.493	39.705	6.944	0.805
7	47.86	9.29	15	3	85.233	39.866	6.938	0.803
8	47.65	10.47	15	3.06	85.627	39.862	6.927	0.800
9	47.38	9.3	14.86	3	83.894	40.101	6.887	0.791

10	47.27	12.51	15	3	85.994	39.763	6.907	0.790

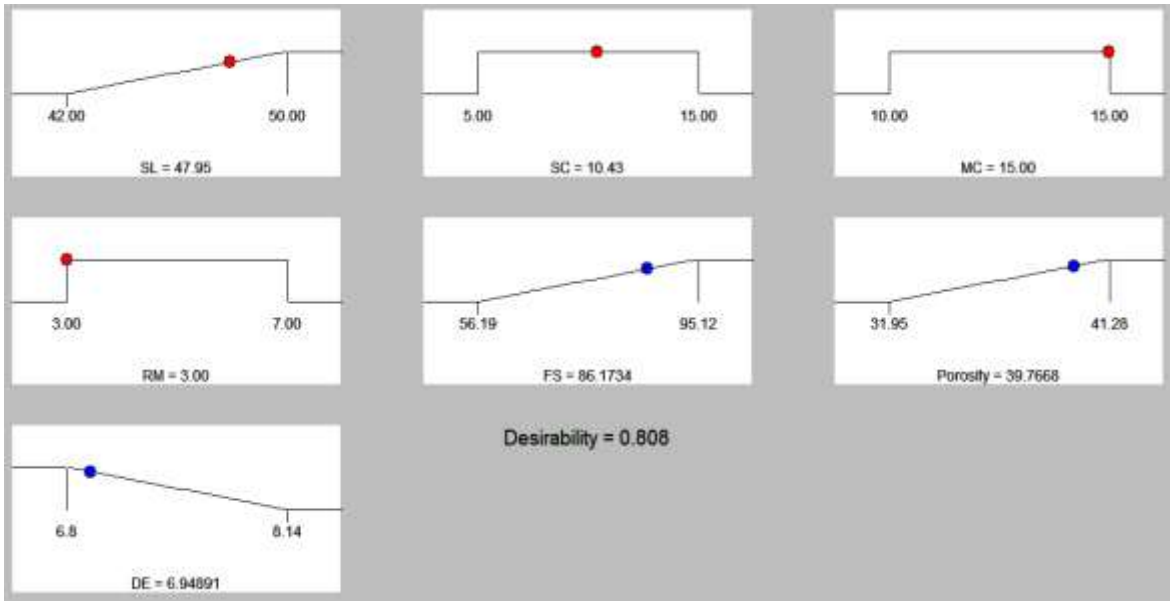

Figure 11. Ramp graphs of desirability function for SiO_2–Si_3N_4 ceramic composite

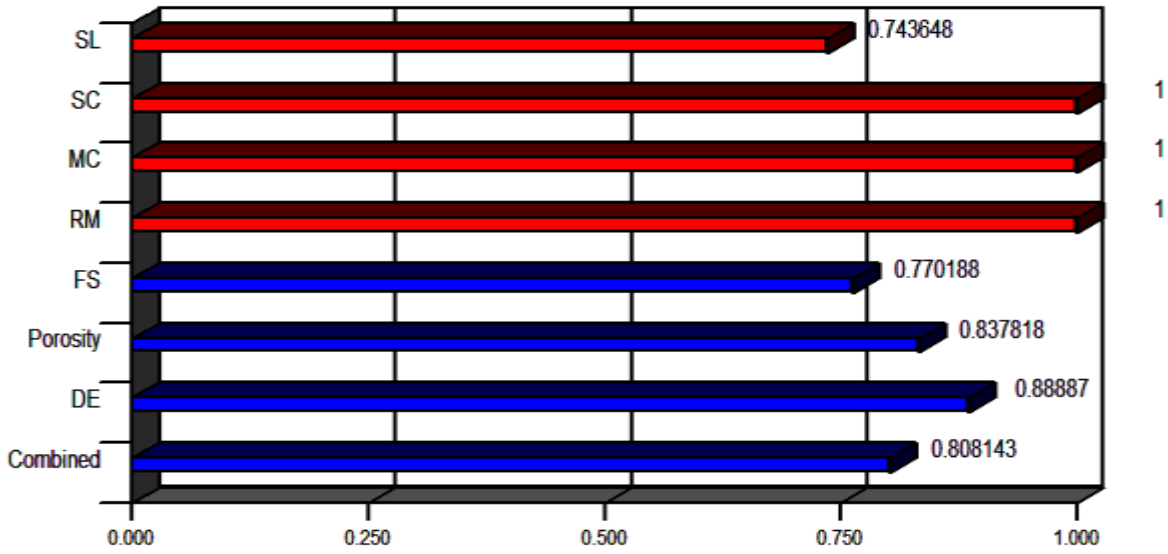

Figure 12. Bar graphs of desirability function for SiO_2–Si_3N_4 ceramic composite

Table 5.24. Error between experimental and predicted values

Run order	SL (vol %)	Si_3N_4 (wt %)	MC (wt %)	RM	Flexural Strength (MPa)			Porosity (%)			Dielectric Constant (K)		
					Expt.	Pred.	Error	Expt.	Pred.	Error	Expt.	Pred.	Error
1	42	5	10	3	56.19	54.98	2.15	37.53	37.71	-0.48	7.22	7.20	0.21
2	46	10	12.5	7	83.16	81.06	2.53	37.18	37.98	-2.15	7.32	7.10	3.06
3	50	15	10	3	92.66	92.24	0.46	32.61	32.09	1.59	7.81	7.78	0.37
4	42	15	10	3	67.89	67.35	0.79	38.41	38.58	-0.45	6.95	6.96	-0.11
5	46	5	12.5	5	75.02	76.46	-1.92	34.16	35.20	-3.04	7.71	7.65	0.78
6	42	5	15	3	58.13	59.49	-2.34	40.36	40.32	0.09	6.82	6.79	0.39
7	42	15	15	7	70.69	71.37	-0.97	38.94	38.46	1.24	6.89	6.95	-0.90
8	46	10	12.5	5	82.67	80.59	2.51	37.67	37.05	1.64	7.29	7.39	-1.40
9	46	10	12.5	3	76.15	78.32	-2.85	39.82	39.36	1.16	6.85	6.95	-1.49
10	42	15	15	3	69.15	68.95	0.29	41.28	41.20	0.20	6.80	6.79	0.20
11	46	15	12.5	5	85.16	84.79	0.44	35.87	35.17	1.96	7.72	7.66	0.80
12	50	5	15	7	89.36	90.22	-0.97	35.13	34.38	2.13	7.76	7.77	-0.14
13	50	15	15	7	93.88	94.50	-0.66	33.15	33.45	-0.90	7.81	7.78	0.44
14	46	10	12.5	5	80.98	80.59	0.48	36.59	37.05	-1.27	7.35	7.39	-0.58
15	50	15	10	7	95.12	94.09	1.09	31.95	32.07	-0.39	8.14	8.17	-0.41

6. Conclusions

The following conclusions were drawn from the present work

- Fused Silica (SiO_2) based ceramic composites SiO_2–Si_3N_4 have been successfully produced using gelcasting method.

- The rheological behavior of the SiO_2 suspensions including SiO_2–Si_3N_4 by varying dispersant content, pH value and solid loading has been thoroughly studied and useful ranges of solid loading (SL), monomer content (MC), ratio of monomers (RM) and Si_3N_4 contents were decided based on initial experiments and they are as follows.

    i. Solid loading: 42 to 50 vol% for SiO_2–Si_3N_4
    ii. Monomer content: 10 to 15 wt%
    iii. Ratio of monomers: 3 to 7
    iv. Si_3N_4 content: 5 to 15 wt%

- Darvan 821A is recommended as a dispersant and a dosage of 0.5 wt% showed better results over other dispersants in the suspension of ceramic particles as 0.5 wt% Darvan 821A gives the maximum zeta potential value for all SiO_2 suspensions.

- The regression models for the analysis of responses such as flexural strength, porosity, and dielectric constant are developed and the effects of the process parameters on these responses are studied.

- The optimum process parameters for maximum flexural strength, maximum porosity, and minimum dielectric constant were evaluated using RSM coupled with desirability function to optimize multiple responses.

- The values of responses i.e. flexural strength, porosity and dielectric constant obtained by experimental runs are compared with predicted regression models for flexural strength, porosity and dielectric constant for SiO_2–Si_3N_4 ceramic composites.

References

1. Li, D., Zhang, C., Li, B., Cao, F., Wang, S., Yang, B.and Liu, K. (2012), "Effects of oxidation treatment on properties of SiO_{2f}/SiO_2-BN composites," *J. Cent. South Univ.*, 19, 30–35.
2. Li, F., Chen, H.Y., Wu, R.Z. and Sun, B.D. (2004), "Effect of polyethylene glycol on the surface exfoliation of SiC green bodies prepared by gelcasting", *Mater. Sci. Eng. A*, 368, 255–259.
3. Wan, W., Huang, C., Yang, J., Zeng, J., and Qiu,T. (2014a), "Effect of Sintering Temperature on the Properties of Fused Silica Ceramics Prepared by Gelcasting", *Journal of Electronic Materials*, 43, 2566-2572.
4. Haris, J. N. and Welsh, E. A. (1973), Fused Silica Design Manual, AD-766494.
5. Jong, B.W., Slavens, G.J. and Traut, D.E. (1992) "Synthesis of silicon and silicon nitride powders by vapour-phase reactions", *Journal of Materials Science*, 27(22), 6086–6090.
6. Chen, F., Shen ,Q. and Zhang, L. (2010), "Electromagnetic optimal design and preparation of broadband ceramic radome material with graded porous structure," *Prog. Electromagn. Res.*, 105, 445-461.
7. Greil, P. (1989), "Processing of silicon nitride ceramics," *Mater. Sci. Eng.*, 109, 27-35.
8. Omatete, O.O., Janney, M.A. and Nunn, S.D. (1997), "Gelcasting: From laboratory development toward industrial production", *J. Eur. Ceram. Soc.*, 17, 407-413.
9. Omatete, O.O., Janney, M.A. and Strehlow, R.A. (1991), "Gelcasting - a new ceramic forming process", *American Ceramic Society Bulletin*, 70, 1641-1649.
10. Nojoomi, A., Faghihi-Sani, M.A. and Khoshkalam, M. (2014), "Shear-rate dependence modeling of gelcast slurries: Effects of dispersant content and solid loading", *Ceram. Int.*, 40, 123–128.
11. Wan, W., Yang, Zeng, J., Yao, L. and Qiu T. (2014), "Effect of solid loading on gelcasting of silica ceramics using DMAA", *Ceram. Int.*, 40, 1735–1740.
12. Wan, W., Yang, J., Qiu,T. and Huang, C. (2014b), "Study on Gelcasting of Fused Silica Glass Using Glutinous Rice Flour as Binder", *International Journal of Applied Glass Science*, 5, 401–409
13. Manivannan, R., Anil Kumar, and Subrahmanyam, Ch. (2013), "Aqueous Gelcasting of Fused Silica Using Colloidal Silica Binder", J. Am. Ceram. Soc., 96, 2432-2436.

14. Mao, X, Wang, S. and Shimai S. (2006), "Preparation of Porous Silica Ceramics with Low Dielectric Constant", *Chinese Journal of Aeronautics*, 19, S239-S243.
15. Lin, S., Ye, F., Ma, J., Ding, J., Yang, C. and Dong, S. (2016), "Fabrication of multilayer electronic magnetic window material by Si_2N_2O decomposition", *Materials and Design*, 97, 51–55.
16. Jia, D.C., Zhou, Y. and Lei, T.C. (2003), "Ambient and elevated temperature mechanical properties of hot-pressed fused silica matrix composite', *J. Eur. Ceram. Soc.*, 23, 801–808.
17. Zou, C., Zhang, C., Li, B., Cao, F. and Wang, S. (2012), "Improved properties and microstructure of porous silicon nitride/silicon oxide composites prepared by sol–gel route", *Materials Science & Engineering A*, 556, 648–652.
18. Li, X., Yin, X., Zhang, L., Cheng, L. and Qi, Y. (2009), "Mechanical and dielectric properties of porous Si_3N_4–SiO_2 composite ceramics", *Mater. Sci. Eng. A*, 500, 63–69.
19. Ganesh, I. and Sundararajan, G. (2010), "Hydrolysis-induced aqueous gelcasting of β-SiAlON–SiO2 ceramic composites: The effect of AlN additive," *J. Am. Ceram. Soc.*, 93, 3180–3189.
20. Montgomery, D.G. (2012), "Design and Analysis of Experiments", 8th edition, John Wiley & Sons, New York, USA.
21. Box, G. E. P., and Draper, N. R. (1987), "Empirical Model Building and Response Surfaces", John Wiley & Sons, New York, NY.
22. Punugupati, G., Bose, P. S. C., Raghavendra, G., & Rao, C. S. P. (2020). Response surface modeling and optimization of Gelcast fused silica micro hybrid ceramic composites. *Silicon*, *12*(7), 1513-1528.